Laboratori Nazionali di Frascati

LNF-73/20

V. Rossi, A. Piazza, G. Susinno, F. Carbonara, G. Gialanella, M. Napolitano, R. Rinzivillo, L. Votano, G. C. Mantovani, A. Piazzoli and E. Lodi-Rizzini:

ANALYSIS OF THE REACTION $\gamma + n \rightarrow p + \pi^-$ IN THE FIRST AND SECOND RESONANCE REGIONS.

Nuovo Cimento 13A, 59 (1973)

IL NUOVO CIMENTO VOL. 13 A, N. 1 1 Gennaio 1973

Analysis of the Reaction $\gamma+n \to p+\pi^-$ in the First and Second Resonance Regions.

V. ROSSI

Istituto di Fisica dell'Università - Roma
Istituto Nazionale di Fisica Nucleare - Sezione di Roma

A. PIAZZA (†) and G. SUSINNO

Laboratori Nazionali del CNEN - Frascati

F. CARBONARA, G. GIALANELLA, M. NAPOLITANO, R. RINZIVILLO and L. VOTANO

Istituto di Fisica dell'Università - Napoli
Istituto Nazionale di Fisica Nucleare - Sezione di Napoli

G. C. MANTOVANI, A. PIAZZOLI and E. LODI-RIZZINI

Istituto di Fisica dell'Università - Pavia
Istituto Nazionale di Fisica Nucleare - Gruppo di Pavia

(ricevuto il 23 Giugno 1972)

Summary. — The final results of an experimental investigation of the reaction $\gamma+n \to p+\pi^-$ performed with a deuterium bubble chamber at the 1 GeV Frascati electrosynchrotron are presented. Total and differential cross-sections on neutrons are extracted by means of the spectator model, the reliability of which has been checked by numerous tests and is extensively discussed. The problems of a possible isotensor component in the electromagnetic current, the time-reversal invariance of the electromagnetic interactions and the photoproduction of the Roper resonance are considered in detail.

(†) Deceased (through a sudden death on the 6-th of August 1972).

1. – Introduction.

The amount of experimental data on single photoproduction processes is at present sufficiently large for π^+ and π^0 photoproduction on protons and the phenomenological analysis of these reactions is rather satisfactory in the low-energy range. On the contrary the experimental data for π^- photoproduction on neutrons are, in this respect, still insufficient and, moreover, the use of the deuteron as a target makes some authors doubt the interpretation of the few results available.

In the present paper we report the results of an experimental investigation of the reaction

$$\gamma + n \to p + \pi^- \tag{1}$$

up to 1 GeV, performed at the Frascati electronsynchrotron with a deuterium bubble chamber.

In the preliminary results [1] we observed some remarkable differences between the proton and neutron total cross-sections in the so-called second-resonance region ($(600 \div 800)$ MeV), suggesting the presence of difference resonant contributions in the two channels. The different position of the bump in the total cross-sections and the results of a simplified phenomenological fit of the angular distributions indicated the presence of a $P_{11}(1470)$ contribution larger than that of the $D_{13}(1520)$, which dominates the π^+ photoproduction process in the same energy region.

This fact, if confirmed, has some nontrivial consequences on the problem of the classification of resonances in the SU_3 scheme.

Moreover the comparison of π^+ and π^- total cross-sections in the first-resonance region may indicate the presence of an isotensor part in the electromagnetic current. Finally, the comparison between the results of reaction (1) and of the inverse one (π^- radiative capture) may give some direct information about the time-reversal properties of the electromagnetic interactions.

Clearly a detailed investigation of the reaction (1) is important not only in view of phenomenological description of the photoproduction processes but also for the more general questions which are involved. The present paper is

---

(1) E. LODI-RIZZINI, G. C. MANTOVANI, A. PIAZZOLI, L. FIORE, G. GIALANELLA, V. ROSSI, A. PIAZZA, G. SUSINNO, F. CARBONARA, M. NAPOLITANO and R. RINZIVILLO: *Lett. Nuovo Cimento*, **3**, 697 (1970); F. CARBONARA, L. FIORE, G. GIALANELLA, M. NAPOLITANO, R. RINZIVILLO, A. PIAZZA, G. SUSINNO, E. LODI-RIZZINI, G. C. MANTOVANI, A. PIAZZOLI, V. ROSSI and L. VOTANO: *Lett. Nuovo Cimento*, **2**, 1183 (1971); A. PIAZZA, G. SUSINNO, L. FIORE, G. GIALANELLA, E. LODI-RIZZINI, G. C. MANTOVANI, A. PIAZZOLI, F. CARBONARA, G. PALOMBA-NICODEMI and R. RINZIVILLO: *Lett. Nuovo Cimento*, **3**, 403 (1970).

divided into six Sections. In Sect. **2** the experimental procedure is briefly described. In Sect. **3** the problem of the use of the deuteron as a target is considered in detail. In Sect. **4** the total and differential cross-sections are presented. In Sect. **5** some considerations on the results concerning the possible T-violation and isotensor current contribution, a phenomenological fit to the differential cross-sections and the $P_{11}(1470)$ photoproduction are reported. Conclusions are given in Sect. **6**.

2. – Experimental apparatus and procedure.

We have analysed 500 000 pictures obtained by exposing the CERN 30 HBC (suitably modified in order to run with deuterium) to the hardened 1 GeV bremsstrahlung beam at the Frascati electronsynchrotron.

The experimental lay-out is the same as in a foregoing experiment ([2]).

The photon flux and the photon spectrum were determined by counting and measuring a sample of e^+e^- pairs in the fiducial volume of the chamber. In Fig. 1 the measured spectrum is shown.

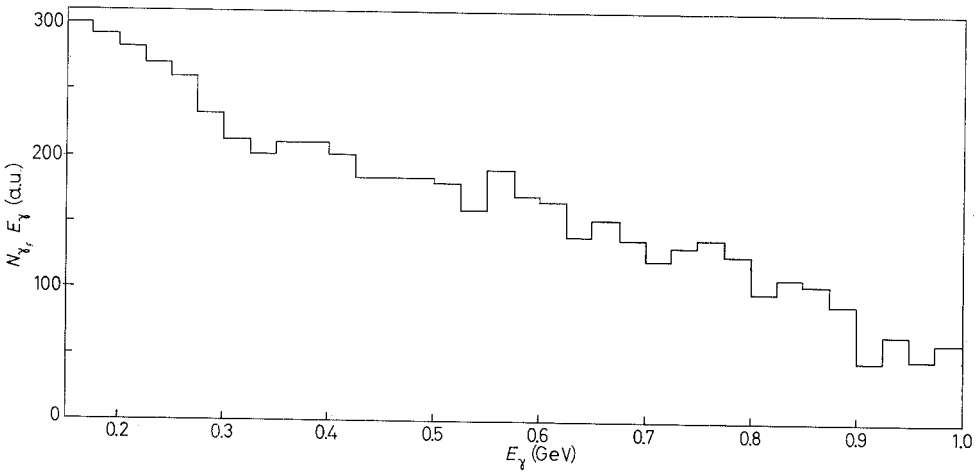

Fig. 1. – Incident-photon spectrum in the laboratory system, as obtained by e^+e^- measurements.

The actual measured reaction is $\gamma+d\to p_s+p+\pi^-$, where p_s is the spectator proton, which is assumed to be the one with the lower momentum. The events were fitted kinematically with three constraints. When the spectator

([2]) G. GIALANELLA, A. PIAZZA, G. SUSINNO, L. FIORE and G. C. MANTOVANI: *Nuovo Cimento*, **63** A, 892 (1969).

proton was not visible ($p_s \leqslant 80$ MeV/c), the usual assumption was made:

$$p_x = p_y = p_z = 0 \text{ and } \Delta p_x = \Delta p_y = 30 \text{ MeV/c}, \ \Delta p_z = 41 \text{ MeV/c},$$

and a 3-C fit was again possible. In Table I the number of events for each of the observed reactions is reported (*).

TABLE I.

Reaction	Number of events
$\gamma+d \to p_s+p+\pi^-$	17384
$\gamma+d \to p_s+p+\pi^-+\pi^0$	1379
$\gamma+d \to p_s+n+\pi^++\pi^-$	2198
$\gamma+d \to n_s+p+\pi^++\pi^-$	2015
$\gamma+d \to d+\pi^++\pi^-$	239

3. – The use of the deuteron as a neutron target.

3·1. *Impulse approximation and spectator model.* – As is always necessary, when studying a reaction on neutrons, we used the deuteron as a target in our investigation of the reaction (1).

The most general way to get the cross-sections on free nucleons using deuterium data is provided by the Chew-Low (3) method, which consists of extrapolating the differential cross-section $\partial^2\sigma/\partial E^{*2}\partial p_s$ to the neutron pole, σ being the cross-section on deuterons, E^{*2} the total squared energy of the π^-p final state and p_s the momentum of the slower proton. However, since the shape of the extrapolation curve is not known, one must have very high statistics for the lowest values of p_s in order to make a linear extrapolation meaningful. Moreover, the results obtained may be affected by the uncertainty in the determination of the unseen spectator momentum ($p_s \leqslant 80$ MeV/c). Unfortunately, this is just the momentum region which is important for the extrapolation, so this method is not very powerful in a bubble chamber experiment with less than a 4-constraint kinematical fit.

Assuming the impulse approximation (4) (I.A.) to hold for a suitably selected sample of events, we have been able to determine the photoproduction cross-

(*) For the criteria adopted for the event assignment to the various reactions see ref. (1).

(3) G. F. CHEW and F. E. LOW: *Phys. Rev.*, **113**, 1640 (1959).

(4) G. F. CHEW and G. C. WICK: *Phys. Rev.*, **85**, 636 (1952); G. F. CHEW and M. L. GOLDBERGER: *Phys. Rev.*, **87**, 778 (1952).

sections on free neutrons by applying the nucleon spectator model in the kinematical calculations, *i.e.* i) we considered the diagram of Fig. 2 as dominant, ii) we assumed the cross-section on the off-mass-shell nucleon to be the same as on a free nucleon, iii) we assumed the total cross-section to depend only on the final-state (π^-p) c.m. energy.

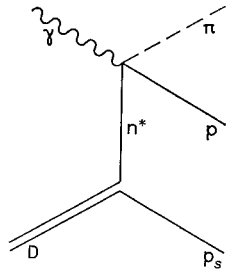

Fig. 2. – Diagram assumed to describe the reaction (1), according to the spectator model.

The limits of validity of the I.A. in the case of the deuteron have been discussed for a long time and all data on neutrons are evidently influenced by them.

Beyond these intrinsic limits, some corrections should in any case be introduced into the experimental data for

i) the so-called Glauber effects [5], *i.e.* shadow and multiple scattering effects;

ii) the Coulomb interaction in the final state [6];

iii) the Pauli principle, which reduces the available phase space;

iv) other final-state interactions of the outcoming particles.

All these effects, which are expected to decrease with the energy, cannot be exactly calculated. An overall evaluation of these corrections may be achieved by the comparison of experimental results referring to the same reaction on free and bound protons. However, the evaluations so obtained are strongly dependent on the kinematics so that it is not easy to apply them to other reactions.

However the shadow and Coulomb effects are expected to be negligible (less than 1%) in our reaction at least for $E_\gamma \geqslant 200$ MeV.

---

[5] R. J. GLAUBER: *Phys. Rev.*, **100**, 242 (1955); F. FRANCO and R. J. GLAUBER: *Phys. Rev.*, **142**, 1195 (1966).

[6] A. BALDIN: *Nuovo Cimento*, **8**, 569 (1958).

The correction for the Pauli principle may be calculated only in a model-dependent way. For example, analysing the same reaction, the ABHHM collaboration (7) used the method of ref. (8) which is able to take into account the Pauli principle if the spin-flip and spin-nonflip amplitudes on neutrons are known. The difference found with respect to the spectator model was of the order of $\sim 6\%$ at most.

As far as the final-state interaction is concerned, one can consider, for example, the π^0 photoproduction on protons in hydrogen and deuterium (9). In that case the observed differences were explained by means of a rescattering process (10).

In ref. (10) the authors give an evaluation of this effect also for the charged-pion photoproduction. The resulting corrections are of the same order as for the above-mentioned Pauli correction, but, below 300 MeV, they go in the opposite sense.

Because of the general uncertainty, we prefer not to consider these corrections in the following.

We will now describe the criteria adopted for the selection of the events and the method used to get the cross-sections on neutrons.

In order to select the sample of events satisfying the spectator model, we made use of a Monte Carlo calculation, which simulates events of reaction (1) in the following way. A photon, extracted from the experimental spectrum, induces the two-step reaction

$$\gamma + \mathrm{D} \to \mathrm{p}_s + \mathrm{Q}, \qquad \mathrm{Q} \to \mathrm{p} + \pi^-$$

according to the spectator model. The spectator momentum p_s is extracted according to the Gartenhaus deuteron wave function and its angular distribution is assumed to be

$$\frac{\mathrm{d}N_s}{\mathrm{d}\Omega} \propto 1 + \beta_s \cos\theta_s ,$$

(7) P. BENZ, O. BRAUN, H. BUTENSCHÖN, H. FINGER, D. GALL, U. IDSCHOK, C. KIESLING, G. KNIES, H. KOWALSKI, K. MÜLLER, B. NELLEN, R. SHIFFER, P. SCHLAMP, H. J. SCHNACKERS, V. SCHULZ, P. SÖDING, H. SPITZER, J. STIEWE, F. STORIM and J. WEIGL: report submitted to the *International Symposium on Electron and Photon Interactions at High Emergies* (Ithaca, N. Y., 1971).

(8) G. F. CHEW and H. W. LEWIS: *Phys. Rev.*, **84**, 779 (1951).

(9) C. BACCI, R. BALDINI-CELIO, B. ESPOSITO, C. MENCUCCINI, A. REALE, G. SCIACCA, M. SPINETTI and A. ZALLO: Frascati Report LNF-72/5 (1972).

(10) R. BALDINI-CELIO and G. SCIACCA: Frascati Report LNF-71/92 (1971).

with β_s, θ_s the spectator velocity and angle in the laboratory system, in order to take into account the Fermi motion in the flux factor (*).

The decay $Q\to p+\pi^-$ is calculated according to the phase-space distribution and, if the resulting proton momentum in the l.s. is lower than that of the spectator, the two protons are interchanged so as to reproduce the choice made for the real events. Moreover, each simulated event is weighted, according to its value of E^{*2} (total c.m. squared energy of the $p\pi^-$ system), with the measured value of the cross-section $\sigma_{\gamma n}(E^{*2})$.

In this way one obtains the distributions of the various quantities of interest, already corrected for all kinematical effects, to be compared with the experimental ones, in particular:

i) the spectator momentum distribution for various E_γ (l.s.) intervals,

ii) the angular distributions of the spectator in the l.s.,

iii) the angular distributions of the spectator in the (γD) c.m.s.

Moreover the Monte Carlo calculation provides suitable correction coefficients for the experimental data due to

i) the wrong choice of the spectator proton,

ii) the loss of the events (one-prong events) in which both protons have a momentum lower than 80 MeV/c,

iii) the cuts introduced in order to select the sample of events satisfying the spectator model (see below).

Finally, if one does not weight the simulated events with the experimental cross-section, one also obtains $N_\gamma(E^{*2})\,dE^{*2}$, *i.e.* the photon spectrum as a function of E^{*2}. This spectrum, which will be used to determine the cross-sections, includes the effects of the kinematical inaccessibility ([11]).

In Fig. 3 and 4 the experimental momentum and angular distributions of the spectator proton for different photon energy intervals (in the l.s.) are shown. The curves are from the Monte Carlo calculation. We want to stress that the different percentages of higher momenta in the various energy intervals are due essentially to a kinematical effect, so that a cut on the spectator momentum does not select in the same way at all energies. For the same reason the spec-

(*) Notice that the cross-section formula $\sigma\propto(n_{ev}/n_{inc})\cdot(1/(v/c))$ contains the ratio between v (the beam relative velocity with respect to the target nucleon, as measured in the l.s.) and c (the beam velocity in the l.s.). If θ is the direction angle of the target nucleon and β its velocity, one has $v/c=\sqrt{1+\beta^2-2\beta\cos\theta}\sim 1-\beta\cos\theta$, and, referring to the spectator nucleon, one sees that each event has to be weighted with a factor $1+\beta_s\cos\theta_s$.

([11]) D. H. WHITE, R. M. SCHECTMAN and B. M. CHASAN: *Phys. Rev.*, **120**, 614 (1960).

tator momentum distribution is not a good index, at least at low energies, for the validity of the spectator model.

A more selective criterion is provided by the angular distribution of the spectator in the overall (γD) c.m.s. These distributions are shown in Fig. 5, for various E_γ intervals.

Since this distribution is expected to be somewhat broadened in a three-body interaction, it seems reasonable to introduce a cut in this angle, which also has the advantage of being slightly correlated to the spectator momentum.

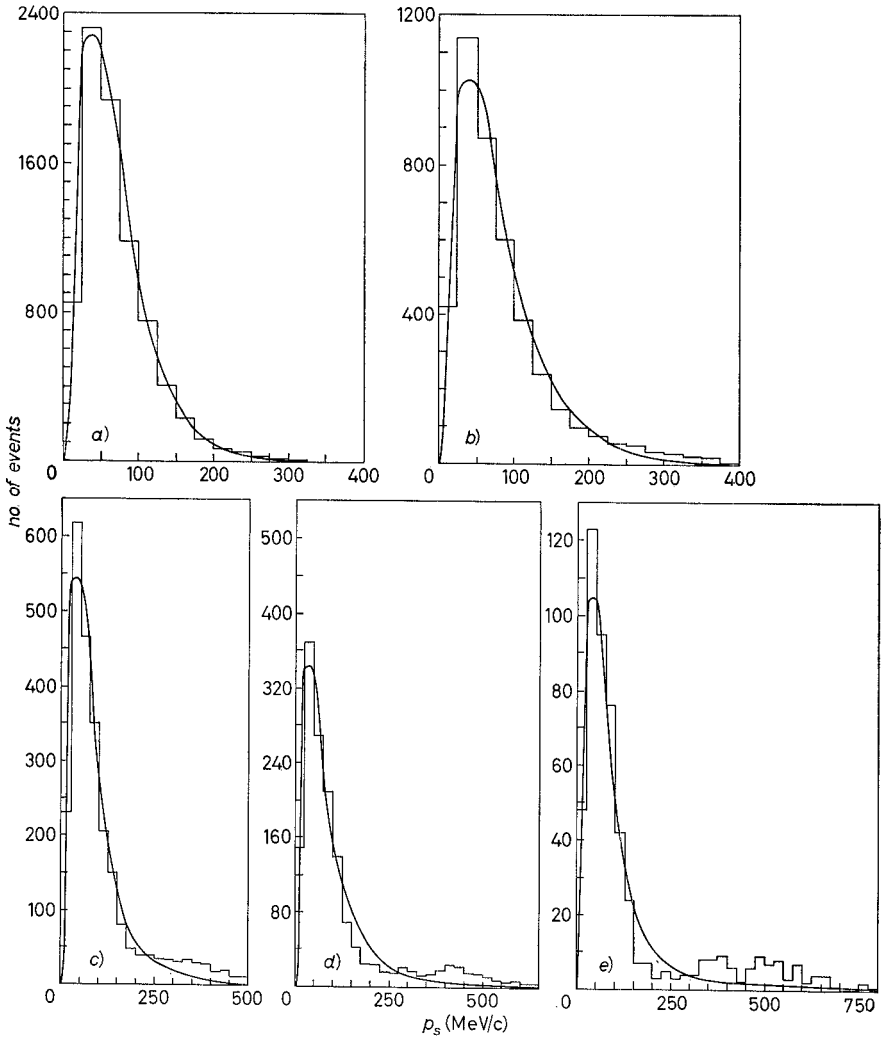

Fig. 3. – Momentum distributions of the spectator proton for various intervals of the photon energy (in the l.s.). The curves show the prediction of the spectator model, including the kinematical effects: *a*) $E_\gamma = (150 \div 300)$ MeV, *b*) $E_\gamma = (300 \div 400)$ MeV, *c*) $E_\gamma = (400 \div 550)$ MeV, *d*) $E_\gamma = (550 \div 750)$ MeV, *e*) $E_\gamma = (750 \div 1000)$ MeV.

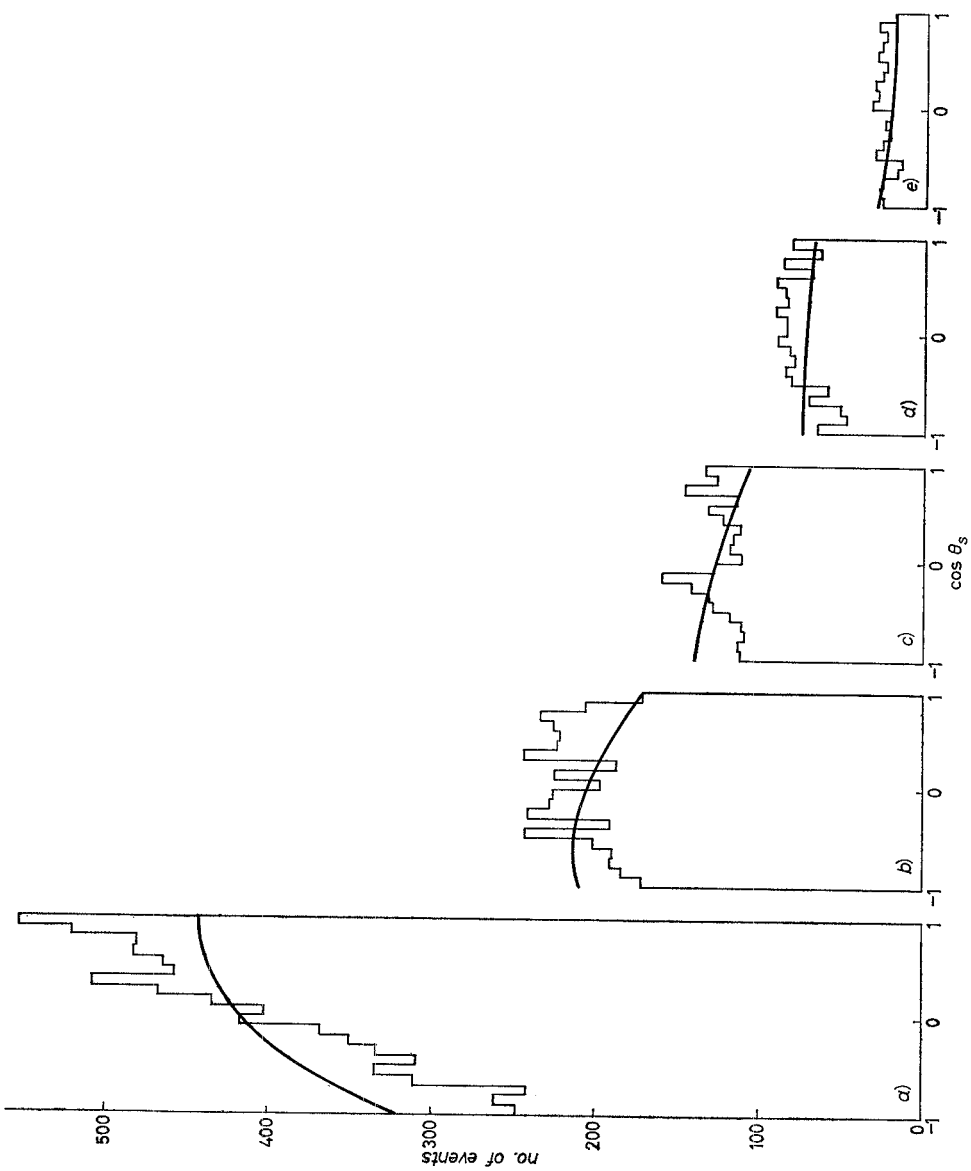

Fig. 4. – Angular distributions of the spectator proton (in the l.s.). The curves show the predictions of the spectator model, including the kinematical effects: *a*) $E_\gamma = (150 \div 300)$ MeV, *b*) $E_\gamma = (300 \div 400)$ MeV, *c*) $E_\gamma = (400 \div 550)$ MeV, *d*) $E_\gamma = (550 \div 750)$ MeV, *e*) $E_\gamma = (750 \div 1000)$ MeV.

Using the spectator model, we have calculated the $\cos\theta_s^*$ distribution. From this prediction we can choose a θ_{0s}^* cut that excludes 5% of the distribution.

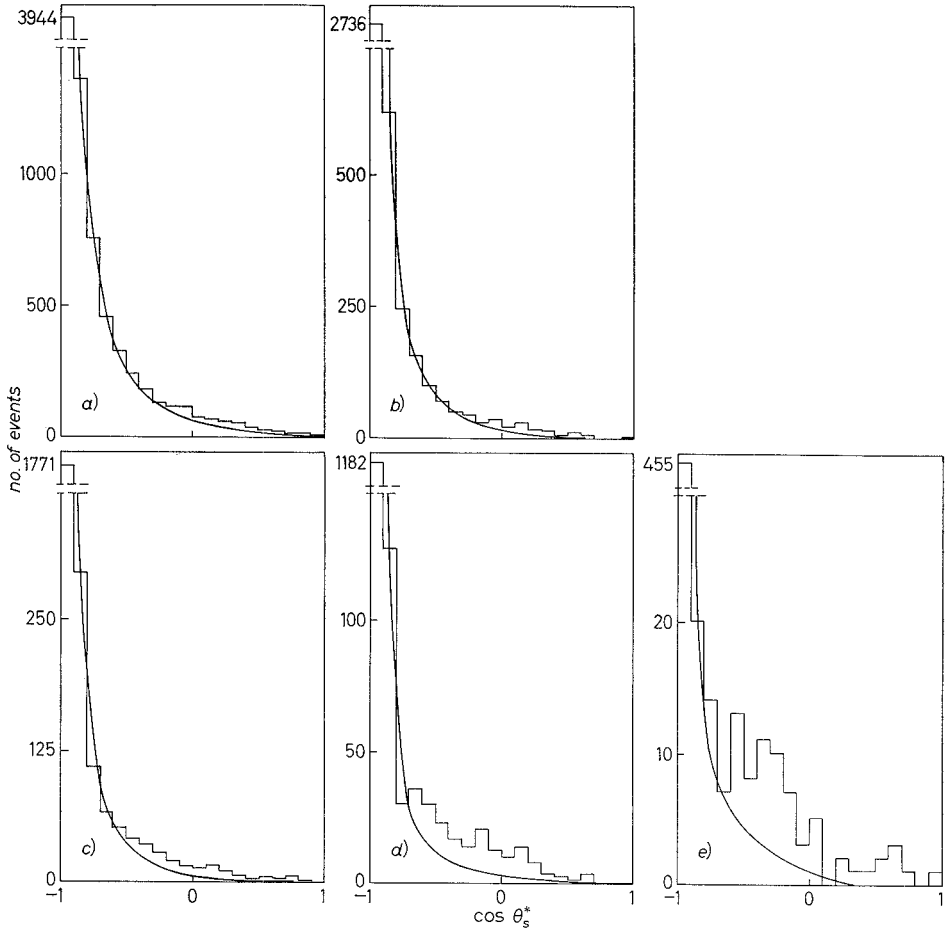

Fig. 5. – Angular distribution of the spectator proton in the γD c.m.s. The curves show the predictions of the spectator model: *a*) $E_\gamma = (150 \div 300)$ MeV, *b*) $E_\gamma = (300 \div 400)$ MeV, *c*) $E_\gamma = (400 \div 550)$ MeV, *d*) $E_\gamma = (550 \div 750)$ MeV, *e*) $E_\gamma = (750 \div 1000)$ MeV.

In Fig. 6 and 7 the momentum and angular distributions of the spectator proton are shown, for values of $\cos\theta_s^*$ higher and lower than the cut value.

The effect of the cut is evident and the agreement between experiment and predictions is now very satisfactory. An interesting feature of this cut is that also events with low spectator momentum can be excluded.

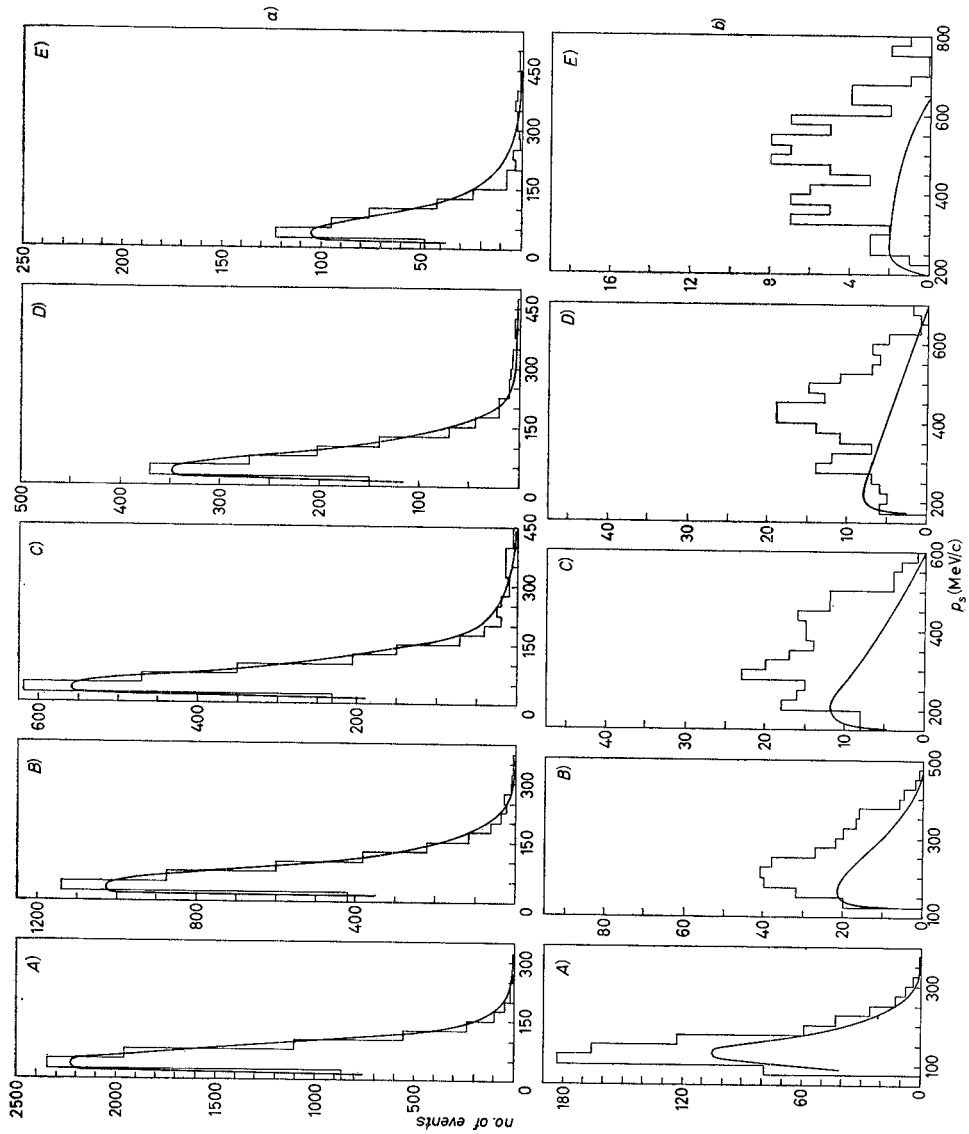

Fig. 6. – Same as Fig. 3, but after the θ_s^* cut: *a*) for $\cos\theta_s^* < \cos\theta_{0s}^*$, *b*) for $\cos\theta_s^* > \cos\theta_{0s}^*$; the curves, representing the predictions of the spectator model, are normalized to the events with $\cos\theta_s^* < \cos\theta_{0s}^*$. *A*) $E_\gamma = (150 \div 300)$ MeV, *B*) $E_\gamma = (300 \div 400)$ MeV, *C*) $E_\gamma = (400 \div 550)$ MeV, *D*) $E_\gamma = (550 \div 750)$ MeV, *E*) $E_\gamma = (750 \div 1000)$ MeV.

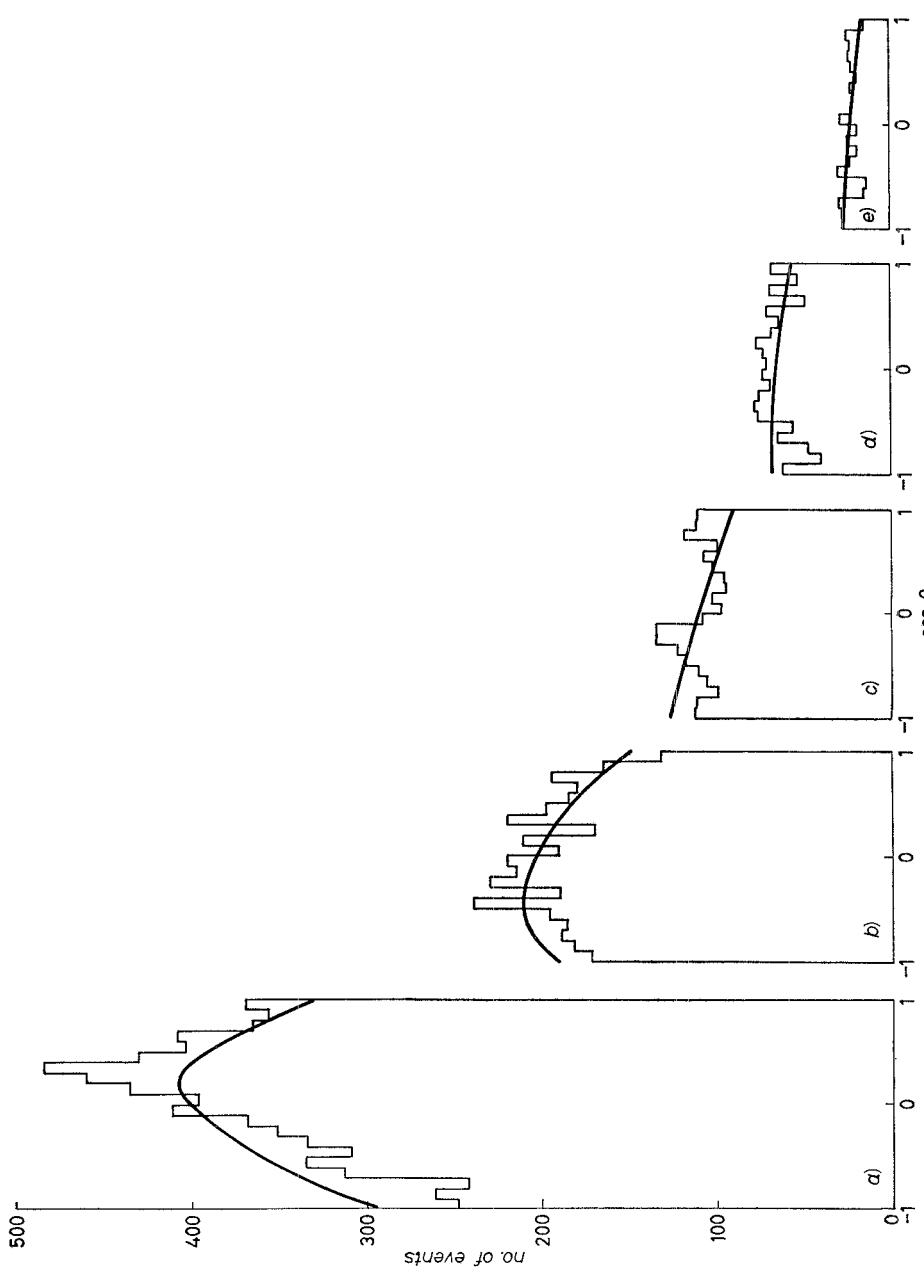

Fig. 7. – Same as Fig. 4, but after the θ_s^* cut: *a*) $E_\gamma = (150 \div 300)$ MeV, *b*) $E_\gamma = (300 \div 400)$ MeV, *c*) $E_\gamma = (400 \div 550)$ MeV, *d*) $E_\gamma = (550 \div 750)$ MeV, *e*) $E_\gamma = (750 \div 1000)$ MeV.

In addition we also introduce the cut on the spectator momentum ($p_s<$ <250 MeV/c), since, above this value, the target nucleon is so far off the mass shell that its interpretation as a free nucleon is scarcely meaningful.

In Table II the percentages of the events which survived the above-mentioned selection criteria and the correction coefficients are given.

TABLE II.

E_γ (MeV)	Number of un-selected events	Number of selected events by θ_s^* cut	Number of selected events by further p_s cut	Fraction of rejected events	Correction coefficients for the two cuts
150÷ 300	7.997	7.290	7.275	0.09	1.06
300÷ 400	4.205	3.920	3.866	0.08	1.04
400÷ 550	2.499	2.279	2.186	0.13	1.07
550÷ 750	1.540	1.352	1.304	0.15	1.07
750÷1000	564	441	429	0.19	1.08

3·2. *Transformation to the neutron rest system.* – Since the γ-n interaction occurs on a target in motion, one has to determine the effective photon energy from the measured quantities.

The first possibility is to do a Lorentz transformation from the l.s. to the neutron rest system, assuming that the neutron momentum before interaction is opposite to the measured spectator momentum ([12]). In this way, however, the mass of the target neutron does not correspond to that of a physical particle.

As an alternative approach ([1]), but again using the spectator model, we have parametrized our results in terms of E^{*2}, the squared c.m. energy of the produced ($p\pi^-$) system. We assumed the effective photon energy E'_γ to be that one necessary to get on a free neutron a total c.m. energy E^* ($E'_\gamma=(E^{*2}-$ $-M_n^2)/2M_n$).

In this way the comparison between the cross-sections on neutrons and protons becomes meaningful.

([12]) H. G. HILPERT, P. LAUSCHER, M. MATZIOLIS, H. SCHNACKERS, H. WEBER, A. MEYER, A. POSE, K. BÖCKMANN, U. IDSCHOK, K. MÜLLER, E. PAUL, E. PROPACH, H. BUTENSCHÖN, H. KÜBECK, D. LÜKE, H. SEEBEK, H. SPITZER, F. STORM, S. BRANDT, O. BRAUN, P. STEFFEN, J. STIEWE, P. SCHLAMP, J. WEIGL and K. WILKINSON: *Nucl. Phys.*, **8** B, 535 (1968); H. BUTENSCHÖN: Desy Report RS-70/1 (1970).

We want to stress that the first approach (Lorentz transformation) gives systematically higher values for the energy than the second one (Fig. 8). This fact produces a misleading shift of the cross-section toward higher energies.

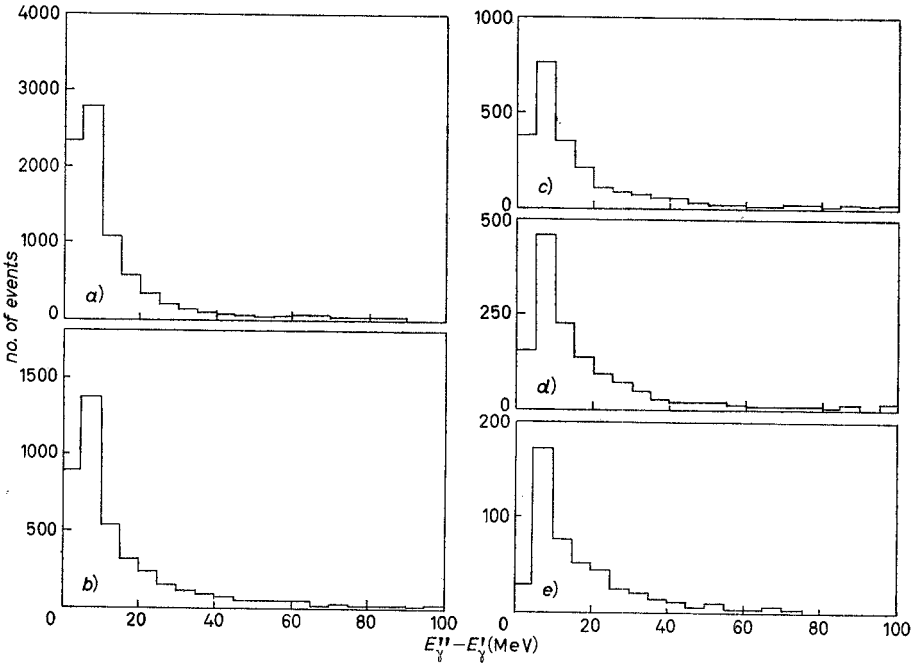

Fig. 8. – Differences between the effective photon energies, as obtained by the Lorentz transformation E''_γ, and the final-state (π^-p) total energy E'_γ (see text), for various E_γ (in the l.s.) intervals: *a*) $E_\gamma = (150 \div 300)$ MeV, *b*) $E_\gamma = (300 \div 400)$ MeV, *c*) $E_\gamma = (400 \div 550)$ MeV, *d*) $E_\gamma = (550 \div 750)$ MeV, *e*) $E_\gamma = (750 \div 1000)$ MeV.

4. – Total and differential cross-sections.

4·1. *Total cross-section* $\gamma + D \to p + p + \pi^-$. – In Fig. 9 we show the total cross-section for the reaction $\gamma D \to pp\pi^-$ *versus* E_γ (l.s.) in order to present the unprocessed experimental results, apart from the obvious corrections of geometrical and instrumental type (scanning efficiency, χ^2 cut, geometrical losses, etc.). The latest values obtained by the ABBHHM collaboration [13] are reported for comparison.

([13]) K. MÜLLER: Bonn University, PIB 3-20 (1971).

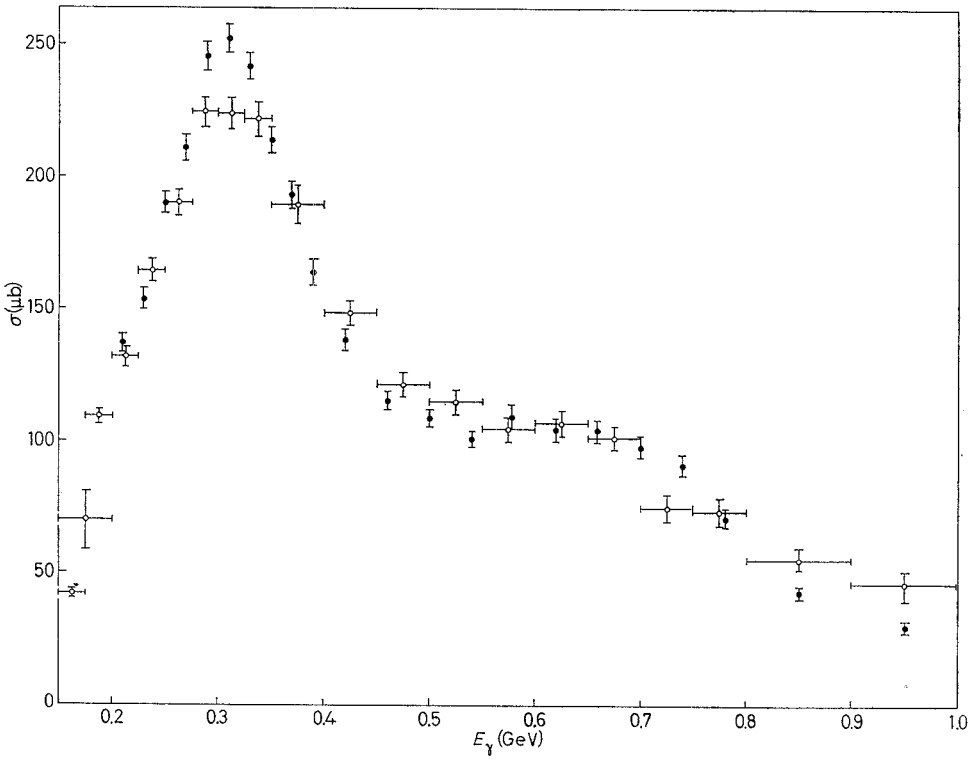

Fig. 9. – Total cross-sections for the reaction $\gamma+D\to p+p+\pi^-$: o this experiment, • ref. [13].

4·2. *Total cross-section* $\gamma+n\to p+\pi^-$. – For the reasons stated in Subsect. 3·1, we assume only those events to be acceptable which verify the two conditions

$$\cos\theta_s^*\leqslant\cos\theta_{0s}^* \qquad \text{and} \qquad p_s\leqslant 250\ \text{MeV/c}\,.$$

The number of events in each E^{*2} interval is then corrected by means of the Monte Carlo calculation. The corrections due to the Pauli principle, shadow and rescattering effects are not introduced for the reasons stated in Subsect. 3·1.

The different energy resolutions for the events and for the photon spectrum measurement are also taken into account.

The resulting total cross-section as a function of E^{*2} (or E'_γ) is shown in Fig. 10 and reported in Table III. The superimposed curves are the cross-sections $\gamma p\to p\pi^0$ and $\gamma p\to n\pi^+$ as obtained from ref. [14]. The quoted errors are purely statistical.

---

[14] J. T. Beale, S. D. Ecklund and R. L. Walker: Report CTSL-42, CALT-68-108.

TABLE III. – $d\sigma/d\Omega^*$ (μb/sr).

E^{*2} $(GeV)^2$	σ (μb)	θ^* (degrees)							
		0 ÷ ÷10	10 ÷ ÷20	20 ÷ ÷30	30 ÷ ÷40	40 ÷ ÷50	50 ÷ ÷60	60 ÷ ÷70	70 ÷ ÷80
1.22 ÷ ÷1.26	132.2 ± ±3.8	—	7.8	2.8	5.5	6.7 ± ±1.0	8.0 ± ±1.0	10.4 ± ±1.1	9.4 ± ±1.0
1.26 ÷ ÷1.30	141.3 ± ±4.2	—	3.5	2.6	2.6 ± ±0.8	5.7 ± ±0.9	7.8 ± ±1.0	9.4 ± ±1.0	10.5 ± ±1.0
1.30 ÷ ÷1.34	182.8 ± ±5.1	—	6.5	3.1	5.6 ± ±1.2	5.9 ± ±1.0	9.1 ± ±1.2	10.8 ± ±1.2	14.6 ± ±1.4
1.34 ÷ ÷1.38	201.0 ± ±5.7	—	1.4	3.5	3.8 ± ±1.0	10.1 ± ±1.4	10.0 ± ±1.3	15.2 ± ±1.5	14.3 ± ±1.5
1.38 ÷ ÷1.42	226.6 ± ±6.5	—	4.3	2.7	4.3 ± ±1.1	5.7 ± ±1.2	9.4 ± ±1.4	14.6 ± ±1.6	18.9 ± ±1.8
1.42 ÷ ÷1.46	250.9 ± ±7.3	—	2.0	3.1	5.7 ± ±1.4	10.4 ± ±1.7	14.8 ± ±1.8	20.5 ± ±2.1	22.2 ± ±2.1
1.46 ÷ ÷1.50	235.1 ± ±7.3	—	2.2	3.4	6.1 ± ±1.5	12.3 ± ±1.9	13.4 ± ±1.8	20.8 ± ±2.2	16.1 ± ±1.9
1.50 ÷ ÷1.54	214.9 ± ±7.4	—	8.4	3.0	7.7 ± ±1.7	11.8 ± ±2.0	13.9 ± ±2.0	21.0 ± ±2.3	20.6 ± ±2.2
1.54 ÷ ÷1.62	188.5 ± ±5.2	—	3.0	7.9 ± ±1.7	8.9 ± ±1.4	13.3 ± ±1.6	13.3 ± ±1.5	14.1 ± ±1.4	17.0 ± ±1.5
1.62 ÷ ÷1.70	141.2 ± ±4.8	—	16.9	6.8 ± ±1.6	9.1 ± ±1.5	14.7 ± ±1.8	12.1 ± ±1.5	11.1 ± ±1.3	13.1 ± ±1.4
1.70 ÷ ÷1.78	111.3 ± ±4.6	—	10.7	8.3 ± ±1.9	6.2 ± ±1.3	9.7 ± ±1.5	10.0 ± ±1.4	10.7 ± ±1.4	13.9 ± ±1.5
1.78 ÷ ÷1.86	102.7 ± ±4.8	—	0	8.9 ± ±2.1	14.3 ± ±2.2	8.5 ± ±1.6	9.1 ± ±1.5	11.3 ± ±1.6	9.4 ± ±1.4
1.86 ÷ ÷1.94	96.6 ± ±4.9	—	6.1	7.9 ± ±2.0	9.7 ± ±1.9	10.1 ± ±1.8	9.3 ± ±1.6	8.6 ± ±1.5	10.2 ± ±1.5
1.94 ÷ ÷2.02	102.7 ± ±5.3	—	3.3	16.5 ± ±3.1	7.9 ± ±1.9	7.5 ± ±1.6	8.4 ± ±1.6	10.9 ± ±1.7	7.9 ± ±1.4
2.02 ÷ ÷2.10	100.4 ± ±5.6	—	9.7	6.5 ± ±2.1	8.5 ± ±2.1	12.1 ± ±2.2	10.5 ± ±1.9	7.3 ± ±1.5	10.1 ± ±1.7
2.10 ÷ ÷2.18	87.3 ± ±5.6	—	3.2	7.3 ± ±2.3	8.8 ± ±2.2	9.3 ± ±2.0	10.4 ± ±2.0	7.3 ± ±1.6	9.1 ± ±1.7
2.18 ÷ ÷2.26	74.1 ± ±5.4	—	7.4	10.0 ± ±2.9	7.5 ± ±2.2	7.1 ± ±1.9	8.3 ± ±1.9	6.7 ± ±1.6	8.5 ± ±1.8
2.26 ÷ ÷2.34	57.5 ± ±5.0	—	1.7	6.3 ± ±2.4	9.4 ± ±2.5	4.9 ± ±1.6	4.2 ± ±1.4	6.0 ± ±1.6	6.0 ± ±1.6
2.34 ÷ ÷2.54	54.8 ± ±3.7	—	2.2	4.7 ± ±1.6	4.7 ± ±1.4	4.8 ± ±1.2	4.1 ± ±1.1	6.0 ± ±1.2	4.5 ± ±1.0
2.54 ÷ ÷2.74	37.9 ± ±4.5	—	7.7	2.1 ± ±1.5	4.7 ± ±1.9	4.4 ± ±1.7	4.4 ± ±1.5	4.5 ± ±1.0	2.8 ± ±1.1

80÷ ÷90	90÷ ÷100	100÷ ÷110	110÷ ÷120	120÷ ÷130	130÷ ÷140	140÷ ÷150	150÷ ÷160	160÷ ÷170	170÷ ÷180
11.3± ±1.0	11.5± ±1.0	10.6± ±1.0	13.0± ±1.2	14.2± ±1.3	12.7± ±1.3	10.8± ±1.3	14.0± ±1.8	12.5± ±2.1	12.0± ±3.6
13.7± ±1.2	12.2± ±1.1	12.8± ±1.2	15.4± ±1.3	13.9± ±1.3	14.4± ±1.5	12.9± ±1.5	14.8± ±1.9	13.9± ±2.4	13.3± ±4.0
15.4± ±1.4	16.9± ±1.5	15.5± ±1.4	19.4± ±1.6	19.2± ±1.7	19.4± ±1.9	21.3± ±2.2	18.8± ±2.4	20.9± ±3.2	21.6± ±5.6
20.2± ±1.7	20.6± ±1.7	19.6± ±1.7	20.6± ±1.8	16.9± ±1.7	22.6± ±2.1	19.8± ±2.2	16.0± ±2.3	17.8± ±3.1	3.3± ±2.3
19.4± ±1.8	23.4± ±2.0	24.0± ±2.0	21.5± ±2.0	23.6± ±2.2	25.9± ±2.5	23.1± ±2.6	25.0± ±3.1	22.1± ±3.8	17.3± ±5.8
27.0± ±2.3	24.2± ±2.1	23.9± ±2.2	23.0± ±2.2	19.4± ±2.1	24.7± ±2.6	26.1± ±2.9	22.0± ±3.2	24.2± ±4.2	17.4± ±6.1
22.7± ±2.2	22.7± ±2.2	22.8± ±2.2	25.2± ±2.4	21.8± ±2.3	25.2± ±2.7	19.6± ±2.7	18.7± ±3.0	24.0± ±4.4	9.5± ±4.8
17.7± ±2.0	16.8± ±2.0	18.7± ±2.1	17.7± ±2.1	19.3± ±2.3	21.4± ±2.9	21.4± ±2.9	20.3± ±3.3	16.1± ±3.8	18.6± ±7.0
16.1± ±1.5	19.9± ±1.6	16.5± ±1.5	14.8± ±1.5	17.7± ±1.7	16.4± ±1.9	16.4± ±1.9	16.0± ±2.2	17.8± ±2.3	10.7± ±4.0
13.0± ±1.4	11.3± ±1.3	13.5± ±1.4	11.6± ±1.4	9.2± ±1.3	9.8± ±1.6	9.8± ±1.6	10.5± ±1.9	7.5± ±2.1	11.9± ±4.5
10.4± ±1.3	11.1± ±1.4	7.4± ±1.1	7.0± ±1.0	7.8± ±1.3	7.9± ±1.5	7.9± ±1.5	6.7± ±1.6	5.8± ±1.9	9.6± ±4.3
8.7± ±1.3	7.7± ±1.2	6.7± ±1.2	7.1± ±1.3	8.4± ±1.2	8.0± ±1.5	7.0± ±1.6	5.2± ±1.6	3.1± ±1.6	6.9± ±4.0
8.5± ±1.4	7.2± ±1.3	7.9± ±1.3	5.4± ±1.2	6.3± ±1.3	5.7± ±1.3	6.2± ±1.6	4.2± ±1.5	6.9± ±2.4	5.1± ±3.6
9.4± ±1.6	8.9± ±1.5	7.3± ±1.4	5.9± ±1.3	9.0± ±1.7	6.8± ±1.6	6.6± ±1.7	6.0± ±1.9	3.9± ±2.0	8.7± ±5.0
7.8± ±1.5	6.9± ±1.4	7.4± ±1.5	5.4± ±1.3	7.3± ±1.6	8.9± ±1.9	7.0± ±1.9	5.4± ±1.9	6.6± ±2.7	6.6± ±4.6
7.0± ±1.4	6.6± ±1.4	6.5± ±1.5	4.2± ±1.2	5.8± ±1.5	9.3± ±2.0	5.5± ±1.7	4.5± ±1.8	2.4± ±1.8	3.6± ±3.6
4.3± ±1.2	6.1± ±1.5	1.5± ±0.7	4.3± ±1.3	7.4± ±1.8	5.6± ±1.7	5.0± ±1.8	3.4± ±1.7	2.8± ±2.0	4.1± ±4.1
1.9± ±0.9	4.6± ±1.3	4.8± ±1.4	5.1± ±1.2	2.4± ±1.0	2.2± ±1.1	4.0± ±1.6	7.3± ±2.6	1.5± ±1.5	4.4± ±4.4
2.7± ±0.8	3.6± ±0.9	2.8± ±0.8	1.5± ±0.6	5.3± ±1.2	4.2± ±1.2	7.1± ±1.7	6.4± ±1.9	10.5± ±3.0	5.2± ±3.7
0.9± ±0.6	0.9± ±0.6	2.3± ±1.0	3.5± ±1.3	2.7± ±1.2	4.4± ±1.7	3.1± ±1.6	2.1± ±1.5	1.7± ±1.7	0

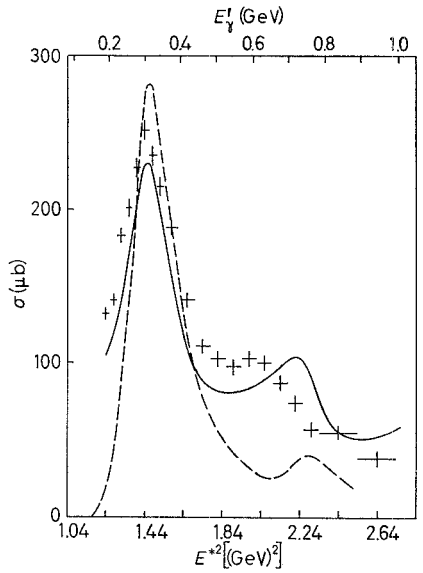

Fig. 10. – Total cross-section for the reaction $\gamma+n\to p+\pi^-$. The superimposed curves are the cross-sections for $\gamma p\to p\pi^0$ (dashed line) and $\gamma p\to n\pi^+$ (full line).

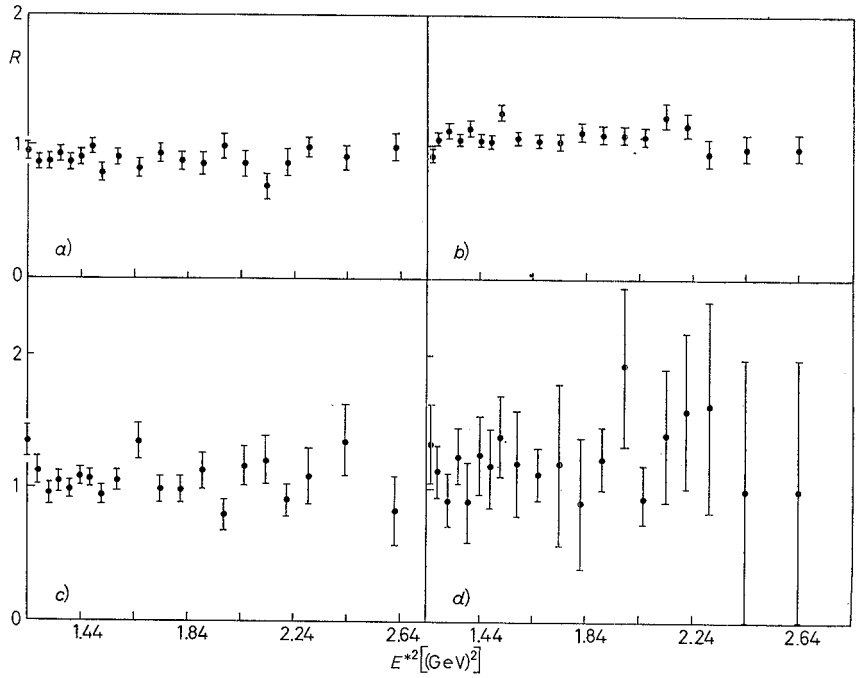

Fig. 11. – Plots of the ratios $R=\sigma(p_{0,250})/\sigma(p_{a,b})$ *vs.* E^{*2}, where $\sigma(p_{a,b})$ is the cross-section value, obtained by the events with $a\leqslant p_s\leqslant b$: *a*) $0\leqslant p_s\leqslant 50$ MeV/c, *b*) $50<p_s\leqslant 100$ MeV/c, *c*) $100<p_s\leqslant 150$ MeV/c, *d*) $150<p_s\leqslant 250$ MeV/c.

We have also checked that the cross-section does not depend very much on the kinematical conditions of the spectator proton. Figure 11 shows the ratios between the total cross-sections for different intervals of the spectator momentum. The fact that this plot is essentially flat assures us that the assumptions we have made are correct.

As already pointed out, the events with $p_s \leqslant 50$ MeV/c give systematically higher values for the cross-sections because the measured spectator momenta are set to zero prior to the kinematical fit and the dispersing effect of the fit itself is not accurate enough.

4·3. *Total cross-section* $\gamma n\to p\pi^-$ *without event selection.* – We want now to determine the total cross-section with the assumption that all the events of the type $\gamma D\to pp\pi^-$ found can be considered as γn events occurring in I.A. This allows us to obtain maximal values for the cross-section on neutrons and to take into account the effect of the Fermi motion without choosing the spectator nucleon.

We want to remark that, apart from the correction factors due to the Pauli principle, this method should correspond to that used in ref. (7), and our results can be compared with those given there.

In order to obtain the cross-section, with this assumption, we proceeded in the following way. The yield of events *vs.* E_γ in the l.s. is transformed into the yield *vs.* E^{*2}, taking into account the Fermi motion by means of a Monte

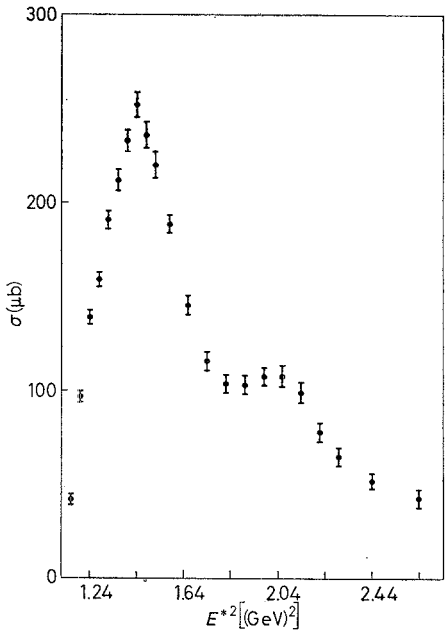

Fig. 12. – A maximal value of the total cross-section with the hypothesis that all the observed $\gamma D\to pp\pi^-$ events could be considered as γn events (see text).

Carlo calculation. This yield combined with the photon spectrum $n_\gamma(E^{*2})\,dE^{*2}$, computed in the same way, gives the required cross-section. This procedure, however, causes a smearing of the cross-section, because for each E_γ value there is a spectrum of E^{*2} values, and consequently it produces a broadening of the first resonance and an apparent shift of the second resonance to higher E^{*2} values.

In order to correct for this effect, we have evaluated the necessary correction coefficients, by doing the comparison, for a sample of simulated events, between the directly calculated E^{*2} distribution and that obtained, with the above procedure, passing through the laboratory energy E_γ.

Figure 12 shows the cross-section obtained, which is only slightly larger, at high E^{*2} values, than that given before. If we remember that the Pauli corrections, as determined in ref. (7), are of the order of 6% at most, it becomes evident that some discrepancies between our results and those of ref. (7) do not depend on the procedure used.

4·4. *Differential cross-sections.* – For the events selected with the criteria stated in Subsect. 2·1, the c.m. angular distributions for twenty E^{*2} intervals

TABLE IV.

E^{*2} $(\mathrm{GeV})^2$	C_0 (μb/sr)	C_1 (μb/sr)	C_2 (μb/sr)	C_3 (μb/sr)
1.22÷1.26	11.4 ± 0.4	-17.9 ± 0.6	4.6 ± 1.1	3.4 ± 0.6
1.26÷1.30	12.9 ± 0.3	-23.0 ± 0.5	6.1 ± 1.9	5.0 ± 0.6
1.30÷1.34	15.9 ± 0.4	-32.1 ± 0.7	14.3 ± 1.1	3.0 ± 0.8
1.34÷1.38	19.7 ± 1.1	-34.7 ± 1.7	6.3 ± 2.9	9.0 ± 2.1
1.38÷1.42	21.5 ± 0.7	-42.8 ± 1.0	16.0 ± 1.7	5.7 ± 1.3
1.42÷1.46	23.8 ± 1.0	-43.6 ± 1.5	12.7 ± 2.6	7.6 ± 2.0
1.46÷1.50	22.9 ± 1.1	-42.2 ± 1.7	11.3 ± 2.9	8.3 ± 2.3
1.50÷1.54	18.8 ± 0.8	-36.1 ± 1.3	14.8 ± 2.2	3.4 ± 1.8
1.54÷1.62	17.6 ± 0.7	-31.3 ± 1.1	7.4 ± 1.8	6.9 ± 1.5
1.62÷1.70	12.6 ± 0.5	-20.7 ± 0.8	2.8 ± 1.4	5.9 ± 1.2
1.70÷1.78	10.0 ± 0.7	-15.2 ± 1.1	-0.2 ± 1.8	5.9 ± 1.6
1.78÷1.86	8.4 ± 0.4	-13.2 ± 0.7	1.7 ± 1.3	3.5 ± 1.1
1.86÷1.94	8.0 ± 0.3	-12.6 ± 0.6	1.1 ± 1.0	3.8 ± 0.8
1.94÷2.02	8.6 ± 0.5	-14.2 ± 0.8	2.3 ± 1.3	3.6 ± 1.1
2.02÷2.10	7.8 ± 0.5	-13.6 ± 0.8	4.5 ± 1.4	1.6 ± 1.2
2.10÷2.18	7.1 ± 0.7	-11.6 ± 1.2	2.2 ± 2.0	2.5 ± 1.7
2.18÷2.26	5.5 ± 0.7	-9.2 ± 1.2	2.7 ± 2.0	1.2 ± 1.7
2.26÷2.34	4.3 ± 0.7	-7.6 ± 1.1	2.8 ± 1.9	7.6 ± 1.7

were determined. They are reported in Table III. The data at small angles, where the corrections (one-prong event) are higher than 25% and the statistics too poor, are given without errors as indicative values.

The experimental distributions were fitted with $\cos\theta^*$ polynomials according to the formula

$$\frac{d\sigma}{d\Omega} = 2\pi(1-\beta\cos\theta^*)^{-2}\sum_{k=0}^{3} C_k \cos^k\theta^* ,$$

where the factor $(1-\beta\cos\theta^*)^{-2}$ is inserted to take explicitly into account the photoelectric term ([15]). For the same reason the cross-section value at the pole, $\cos\theta^* = +1/\beta$, was taken as a constraint in the fit.

In Table IV and in Fig. 13 the coefficients C_k are reported.

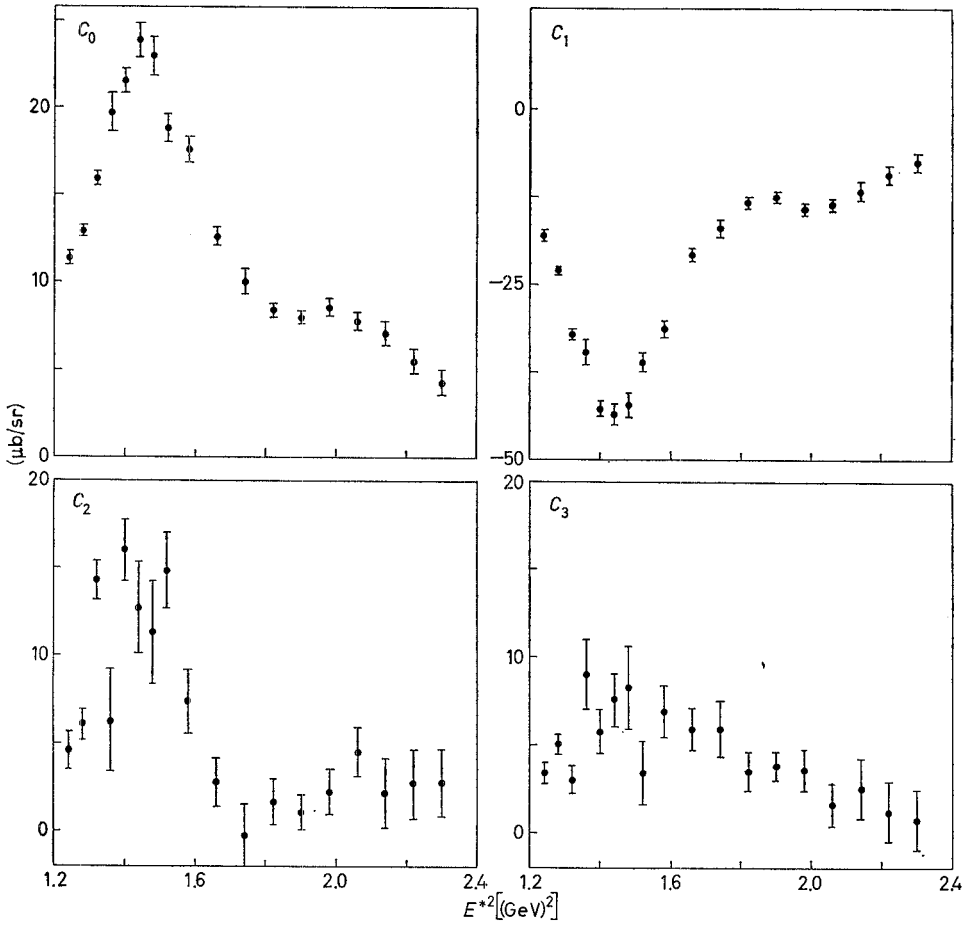

Fig. 13. – Behaviour of the coefficients of the Moravcsik polynomial fit to the angular distributions as a function of E^{*2}.

([15]) M. I. MORAVCSIK: *Phys. Rev.*, **104**, 1451 (1956).

Finally we report a further check on the validity of the spectator model. In Fig. 14 the ratios between the π^- in the backward and in the forward directions are given for different angles and momenta of the spectator proton. As one should expect, for a given E^{*2} interval, this ratio appears to be independent of the kinematical conditions of the spectator proton, thus confirming the overall consistency of the selection criteria adopted.

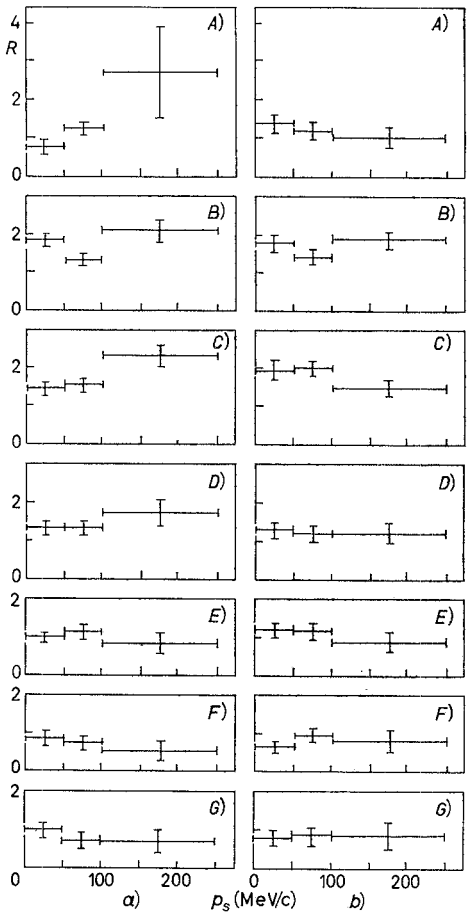

Fig. 14. – Ratios R between the π^- in the backward and in the forward directions (c.m.s.) as a function of p_s: *a*) $\cos\theta_s > 0$, *b*) $\cos\theta_s < 0$. *A*) $E^{*2} = 1.14 \div 1.22$, *B*) $E^{*2} = 1.22 \div 1.38$, *C*) $E^{*2} = 1.38 \div 1.46$, *D*) $E^{*2} = 1.46 \div 1.54$, *E*) $E^{*2} = 1.54 \div 1.74$, *F*) $E^{*2} = 1.74 \div 2.10$, *G*) $E^{*2} = 2.10 \div 2.74$.

5. – Analysis of the results.

In this Section we discuss our data in the light of some very important theoretical questions which have recently come under examination.

5·1. *Isotensor component of the electromagnetic current.* – The comparison of the total cross-sections of the pion photoproduction on protons and neutrons, in the first-resonance region allows us to search for the possible existence of an isotensor term in the e.m. current.

In the past some authors ([16]) emphasized the complete lack of direct experimental proofs for the assumption that in photon induced reactions one should have $\Delta T \leqslant 1$. They suggested performing photoproduction measurements and pointed out that the comparison between the cross-sections for production of the Δ^+ and Δ^0 states of the $P_{33}(1236)$ resonance could throw some light on the question. In effect, if one puts

$$\sigma(\gamma n \to \Delta^0) = \sigma(\gamma p \to \Delta^+)(1 + x^2),$$

from the usual isotopic decomposition ([17]) of the single-photoproduction amplitude (including the isotensor amplitude A_T), x is shown to be zero if $A_T = 0$.

Indeed, if one wants to determine A_T without ambiguities, careful experiments should be done on the four single-photoproduction reactions. At present this is premature and one has to make some assumptions on the reaction mechanism.

In particular, SANDA and SHAW ([18]) assumed the dominance of the P_{33} resonance on the background, almost constant with energy, and calculated, for various x, the quantity

$$A = \frac{K}{q}\left[\sigma_T(\gamma n \to p\pi^-) - \sigma_T(\gamma p \to n\pi^+)\right]$$

by using dispersion relations and the following parametrization of the resonant multipole:

$$nM^{\frac{3}{2}}_{1^+} = pM^{\frac{3}{2}}_{1^+}(1 + x).$$

In Fig. 15 the comparison between the predictions of SANDA and SHAW and the experimental data is shown. The quantity A has been determined by using our data and the π^+ cross-section taken from ref. ([19]).

([16]) V. G. GRISHIN, V. L. LYUBOSHITZ, V. I. OGIEVETSKII and M. I. PODGORETSKII: *Sov. Journ. Nucl. Phys.*, **4**, 90 (1967); B. GITTELMAN and W. SCHMIDT: *Phys. Rev.*, **175**, 1998 (1968); N. DOMBEY and P. K. KABIR: *Phys. Rev. Lett.*, **17**, 730 (1966); G. SHAW: *Nucl. Phys.*, **3** B, 338 (1967); A. DONNACHIE and G. SHAW: *Phys. Lett.*, **35** B, 419 (1971); R. C. E. DEVENISH, D. H. LYTH and W. A. RANKIN: *Nucl. Phys.*, **36** B, 309 (1972).

([17]) F. A. BERENDS and D. L. WEAVER: *Phys. Rev. D*, **4**, 1997 (1971).

([18]) A. I. SANDA and G. SHAW: *Phys. Rev. Lett.*, **24**, 1310 (1970); *Phys. Rev. D*, **3**, 243 (1971); *Phys. Rev. Lett.*, **26**, 1057 (1971).

([19]) P. SPILLANTINI and V. VALENTE: Frascati Report LNF-71/28 (1971).

As one can observe our results are compatible with $x = 0.2$, and an overall upward correction of about 20% to our data would be necessary to cancel this effect. Such an amount certainly cannot be attributed to the deuteron corrections discussed above, which have not been introduced in our results.

We want to remark that some energy dependence of the corrections themselves could somewhat change the experimental A distribution. This fact could be important, because according to SANDA and SHAW, the « dip » behaviour of the A distribution is more indicative than the A absolute values.

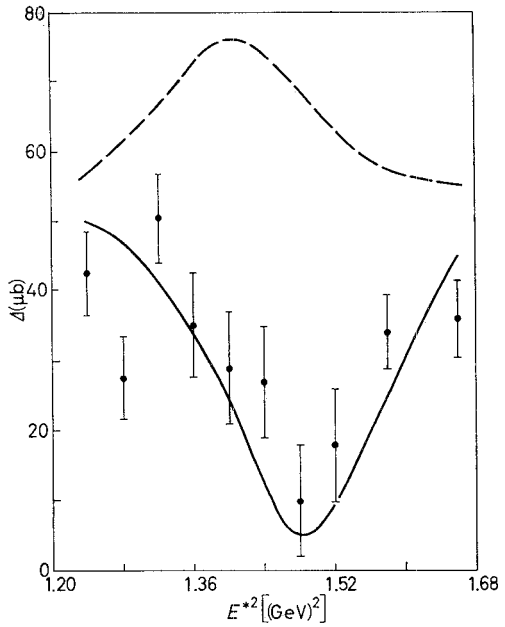

Fig. 15. – $A = q/K\,[\sigma_T(\gamma n \to p\pi^-) - \sigma_T(\gamma p \to n\pi^+)]$ as a function of E^{*2}. The curves are the predictions ([18]) with $x = 0.20$ (full line) and $x = 0$ (dashed line).

5·2. *T-invariance of e.m. current.* – The comparison between the differential cross-sections for π^- photoproduction and its inverse (π^- radiative capture) in the first-resonance region is quite sensitive to a possible T-violation in the e.m. interaction of hadrons ([20]).

In Fig. 16 we report this comparison for three values of E^*, using the available $\pi^- + p \to n + \gamma$ data ([21]), suitably modified by means of the detailed balancing principle. The values for the direct reaction $\gamma n \to p\pi^-$ were calculated using the polynomial fit described in the foregoing Section. The shaded band contains two standard deviations about the calculated values.

([20]) N. CHRIST and T. D. LEE: *Phys. Rev.*, **148**, 1520 (1966).

([21]) P. A. BERARDO, R. P. HADDOCK, B. M. K. NEFKENS, L. J. VERHEY, M. E. ZELLER, A. S. L. PARSONS and P. TRUOEL: *Phys. Rev. Lett.*, **26**, 201 (1971).

There seems to be a satisfactory agreement for energies above the first-resonance region, while at $E^* = 1.245$, our results are noticeably higher than those of the inverse reaction. It is surely premature to draw definitive conclusions on this question, also considering that the inverse reaction requires further investigation because of the problem of the large (π^0n) background.

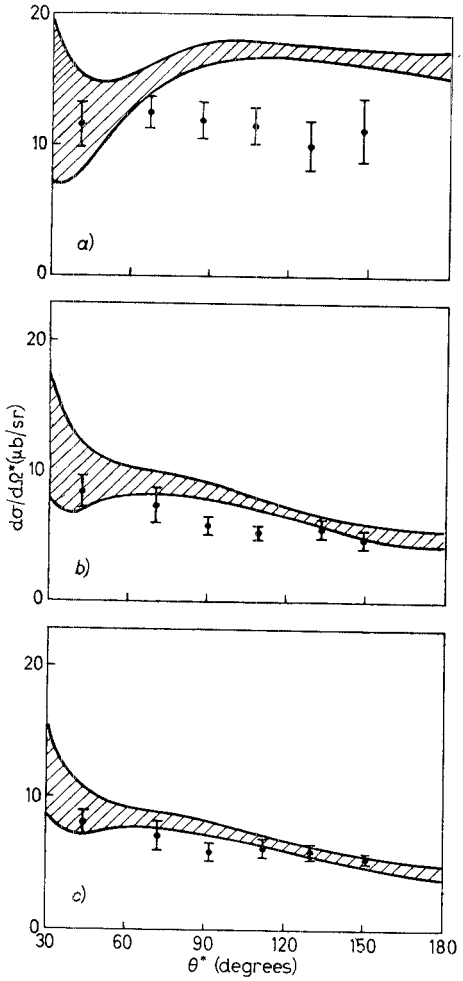

Fig. 16. – Comparison between the differential cross-sections for $\pi^-p\to n\gamma$ (points from ref. ([21])) and $\gamma n\to\pi^-p$ (shaded band): *a*) $E^* = 1.245$ GeV, *b*) $E^* = 1{,}337$ GeV, *c*) $E^* = 1.363$ GeV.

5·3. *Phenomenological fit of the differential cross-sections.* – At present the available data are not sufficient to describe completely the photoproduction processes in terms of a multipole expansion, so that in any phenomenological

analysis one has to apply specific models in order to obtain the behaviour of some multipoles.

By using our experimental angular distributions and making some reasonable assumptions, we carried out a phenomenological fit extending from 0.4 to 0.9 GeV in E'_γ, by means of an isobaric model analogous to that of WALKER [22].

The photoproduction amplitude is assumed to be given by a linear combination of three contributions:

a) resonant amplitudes (in our energy interval we only considered P_{33}, S_{11}, P_{11} and D_{13}),

b) Born terms with electric coupling only,

c) nonresonant background terms.

Furthermore, we have adopted the following criteria:

i) The imaginary part of each amplitude is only due to the resonant contribution which is described by a Breit-Wigner function.

ii) Consequently the nonresonant background terms are added only to the real part of the amplitude. In this way, the fit is mostly sensitive to the resonant contributions. Moreover the background terms are assumed to be constant with energy.

iii) The P_{33} resonant contribution is fixed to the Walker value [22]. This implies that one must consider ${}_nM^{\frac{3}{2}}_{1^+} = {}_pM^{\frac{3}{2}}_{1^+}$, which seems to be irrelevant, since, above 400 MeV, only the tail of the resonance itself intervenes.

iv) In the fit two available polarization [23] and asymmetry [24] results are taken into account.

The fit results have been already published [1] and are quoted in Table V.

We want to stress that the above fit does not claim to give the exact behaviour of the multipoles contributing to the investigated reaction, but only to extract, in the framework of the isobaric model used, the relative importance of the resonant contributions. In this sense one has also to consider the comparisons between our results and those of other fits.

The most interesting result of our fit is the very large $P_{11}(1470)$ contribution with respect to that of $D_{13}(1520)$, which is known to dominate the corresponding reaction on protons. This result is also found in the fit of ref. [25], in which a different parametrization is assumed. Moreover, these authors, starting

---

[22] R. L. WALKER: *Phys. Rev.*, **182**, 1729 (1969).

[23] M. BENEVENTANO, S. D'ANGELO, F. DE NOTARISTEFANI, P. MONACELLI, L. PAOLUZI, F. SEBASTIANI, M. SEVERI and B. STELLA: *Lett. Nuovo Cimento*, **3**, 840 (1970).

[24] K. KONDO, T. NISHIKAWA, T. SUZUKI, K. TAKIKAWA, H. YOSHIDA, Y. KIMURA and M. KOBAYASHI: *Journ. Phys. Soc. Japan*, **29**, 13 (1970).

[25] A. PROIA and F. SEBASTIANI: *Lett. Nuovo Cimento*, **2**, 560 (1971).

TABLE V.

Resonant helicity element	Added contributions	Resonance	Energy W_0 (GeV)	Width Γ_0 (GeV)	$A^-(W_0)$ ($\mu b^{\frac{1}{2}}$)
A_{1+}		P_{33}	1.236	0.120	1.00 (fixed to Walker value)
	A_{1+}				$-0.29^{+0.06}_{-0.07}$
B_{1+}		P_{33}	1.236	0.120	-2.43 (fixed to Walker value)
	B_{1+}				$1.05^{+0.10}_{-0.09}$
A_{2-}		D_{13}	1.519	0.102	$-0.31^{+0.1}_{-0.1}$
	A_{2-}				$-0.36^{+0.07}_{-0.07}$
B_{2-}		D_{13}	1.519	0.102	$-0.16^{+0.16}_{-0.17}$
	B_{2-}				$0.80^{+0.1}_{-0.09}$
A_{0+}		S_{11}	1.561	0.180	$-0.22^{+0.17}_{-0.17}$
	A_{0+}				$0.41^{+0.12}_{-0.09}$
A_{1+}		P_{11}	1.471	0.200	$-1.00^{+0.09}_{-0.09}$
	A_{1-}				$0.65^{+0.11}_{-0.11}$

from the data of the present experiment, are able to derive some predictions for the reaction $\gamma n\to n\pi^0$ which agree with a recent experiment ([26]). The P_{11} contribution found is also in agreement with the predictions of ref. ([27]). In Table VI the comparison among some recent fits ([22,25]) is reported.

TABLE VI.

Resonant helicity element	Resonance	Our results	Walker results, ref. ([22])	Proia-Sebastiani results, ref. ([25])
A_{0+}	S_{11}	-0.22	-0.8	-0.395
A_{1-}	P_{11}	-1.00	0	-0.760
B_{2-}	D_{13}	-0.16	-1.15	-0.258
A_{2-}	D_{13}	-0.31	0	0

5·4. *The* $P_{11}(1470)$ *resonance in photoproduction.* – As already discussed in ref. ([1]), the results of the phenomenological fit support the indication of P_{11} formation which is given by the behaviour of the total cross-section in the

([26]) C. BACCI, R. BALDINI-CELIO, B. ESPOSITO, C. MENCUSSINI, A. REALE, G. SCIACCA, M. SPINETTI and A. ZALLO: *Phys. Lett.*, **39** B, 559 (1972).
([27]) J. BAACKE and H. KLEINERT: *Lett. Nuovo Cimento*, **2**, 463 (1971).

second-resonance region. A backward displacement of the bump, with respect to the corresponding reaction on protons is evident. Both facts suggest that $P_{11}(1470)$ strongly contributes to the photoproduction on neutrons.

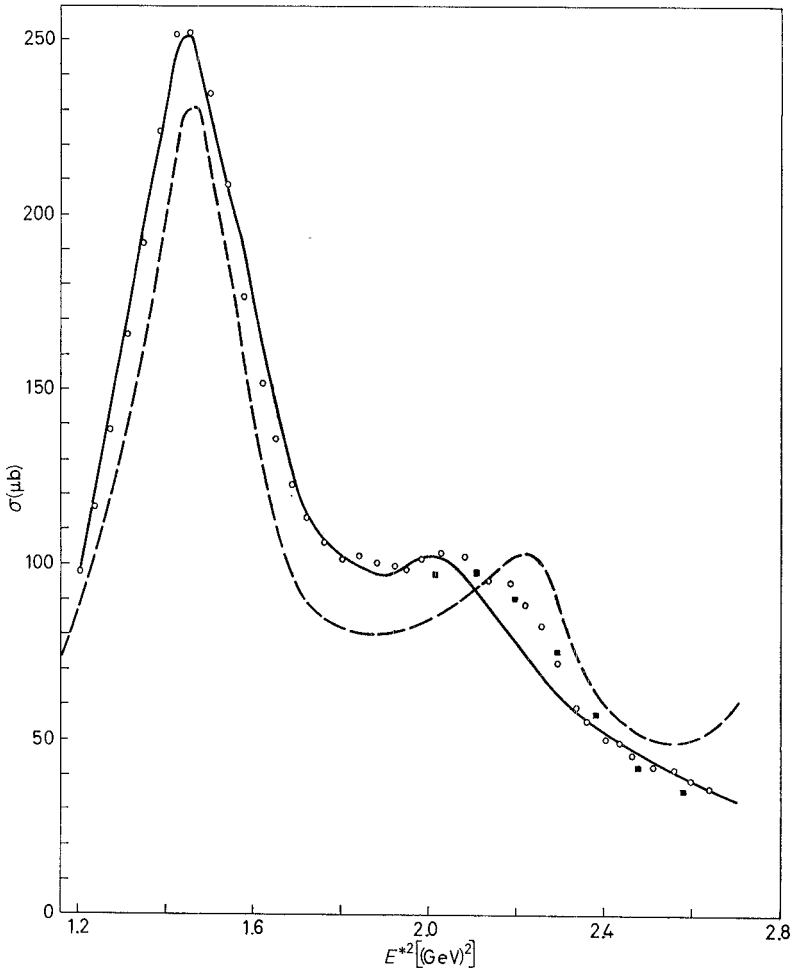

Fig. 17. – Total cross-section of the reaction $\gamma n \to p\pi^-$. The π^+ photoproduction cross section is also reported (dashed line). ——— results of Fig. 10, ■ ref. ([28]), ○ our calculated results for the π^-/π^+ ratio.

Some comparisons have to be made with other experiments which do not seem to show the same result. Concerning the ΔBHHM collaboration experiment performed with the same technique, the extracted γn cross-section shows a bump at higher energy which is attributed to the D_{13}-resonance. In

([28]) P. E. SHEFFLER and P. L. WALDEN: *Phys. Rev. Lett.*, **24**, 952 (1970).

our opinion the discrepancy is mainly due to the difference in the unprocessed data.

As concerns the results of ref. ([28]), obtained with counters by measuring the π^-/π^+ ratio, we want to remark that the cross-section reported by these authors is given as a function of E_γ in the l.s., so that a backward shift of about (20 ÷ ÷30) MeV could be obtained in this energy region, if the E^{*2} energy parametrization was chosen. This feeling is supported by the results of a Monte Carlo calculation in which we determined the π^-/π^+ ratio on deuterons as a function of E_γ (l.s.), using our π^- cross-section and the known π^+ cross-section. By so doing we reproduced the data of ref. ([28]). The comparison is shown in Fig. 17.

Finally we want to point out that the π^-/π^+ ratio ([29]) passes through unity just at 600 MeV, so that one could infer that a bump displacement between the two reactions is present.

These considerations give us sufficient confidence to make a claim for $P_{11}(1470)$ photoproduction in the reactions on neutrons.

If it is confirmed that the same does not happen on protons ([22]), then the P_{11} would belong to an SU_3 antidecuplet, not provided by the simple quark model. This assignment can be confirmed by looking for the decay mode $P_{11}\to\Delta+\pi$ ([30]), which would be forbidden in this case.

This analysis is in progress in double pion photoproduction on neutrons and the preliminary results ([1]) (in apparent disagreement with some previous indications ([31])) seem to confirm the above statement.

6. – Conclusions.

From the data of an investigation of the reaction $\gamma d\to pp\pi^-$ we were able to derive cross-sections for the reaction $\gamma n\to p\pi^-$ by using the spectator model. The events were selected by means of a cut on the spectator angle in the (γD) c.m.s. and on the l.s. momentum of the spectator itself.

Numerous checks assured us of the reliability of the model and of the effectiveness of the selection cuts.

The results can be summarized as follows:

a) If the theoretical model of SANDA and SHAW is reliable, the existence of an isotensor current cannot be excluded by our experimental results, as it is by those of the ABHHM collaboration.

([29]) G. NEUGEBAUER, W. WALES and R. L. WALKER: *Phys. Rev.*, **119**, 1726 (1960).
([30]) H. J. LIPKIN: *Phys. Lett.*, **12**, 154 (1964).
([31]) A. DONNACHIE: *Proceedings of the XIV International Conference on High-Energy Physics* (Vienna, 1968), p. 139.

Our data without Pauli and final-state corrections agree with the value $x = 0.2$ of the isotensor parameter and the above corrections, as far as we presently know, cannot cancel the effect.

Indeed, the difference between our data and those of the ABHHM collaboration appears already in the total deuteron cross-sections, that are unaffected by any deuteron effet. In our opinion, this is the main experimental fact leading us not completely to exclude an isotensor contribution.

However, we want to point out that the Sanda and Shaw test is model dependent, due to the assumptions made on the background behaviour, so our data could also not require an isotensor contribution.

b) If the data on the inverse reaction are reliable, the T-invariance would be violated, both with our data and, even more, with those of the ABHHM collaboration. However, π^- radiative capture is very difficult to be measured and the experimental data on this subject are presently not sure enough. So, we think that T-invariance still remains a completely open problem.

c) The total cross-section shows an enhancement at $E'_\gamma = 580$ MeV, which cannot be easily attributed to the expected $D_{13}(1520)$-resonance, but rather to the $P_{11}(1470)$-resonance, as indicated also by a phenomenological fit to the differential cross-sections.

* * *

We wish to thank all those who made this work possible, in particular the members of our technical staff, Messrs. P. BENVENUTO, A. DELLA CIANA, D. FABBRI, M. GESINI, L. MAIANI, and of the measuring and scanning staff, C. CAIAZZO, A. CASCINI, C. CASELLA, M. CIPRIANO, F. CORTELLESSA, C. DE PALO, E. D'USCIO, M. GATTA, C. LAMBO, A. MONTAGNA, A. PARMENTOLA, C. SOGARO and C. TORNATORE.

● RIASSUNTO

Si presentano i risultati finali di un'indagine sperimentale della reazione $\gamma+n\to p+\pi^-$ eseguita con una camera a bolle a deuterio presso l'elettrosincrotrone da 1 GeV di Frascati. Le sezioni d'urto totali e differenziali sono ricavate usando il modello dello spettatore la cui validità è stata sottoposta a numerosi controlli ed è discussa in dettaglio. Sono considerati in particolare i problemi riguardanti una possibile componente isotensoriale della corrente elettromagnetica, l'invarianza per inversione rispetto al tempo delle interazioni elettromagnetiche e la fotoproduzione della risonanza di Roper.

Анализ реакции $\gamma + n \to p + \pi^-$ в области первого и второго резонансов.

Резюме (*). — Приводятся окончательные результаты экспериментального исследования реакции $\gamma + n \to p + \pi^-$, проведенного на дейтериевой пузырьковой камере при энергии 1 ГэВ на электронном синхротроне Фраскати. Вычисляются полные и дифференциальные поперечные сечения на нейтроне, используя модель наблюдателя, надежность которой подробно обсуждается и была проверена с помощью численных расчетов. Подробно рассматриваются проблемы возможной изотензорной компоненты в электромагнитном токе, инвариантность электромагнитных взаимодействий относительно обращения времени и фоторождение резонанса Ропера.

(*) *Переведено редакцией.*